Probing the Surface Effect on Deep-Level Emissions of an Individual ZnO Nanowire via Spatially Resolved Cathodoluminescence

Haizhou Xue,[†] Nan Pan,*[,†] Rongguang Zeng,[†] Ming Li,[†] Xia Sun,[‡] Zejun Ding,[‡] Xiaoping Wang,*[,†,‡] and J. G. Hou[†]

Hefei National Laboratory for Physical Sciences at the Microscale, University of Science and Technology of China, Hefei, Anhui 230026, P. R. China, and Department of Physics, University of Science and Technology of China, Hefei, Anhui 230026, P. R. China

Received: April 22, 2009; Revised Manuscript Received: May 21, 2009

Spatially resolved cathodoluminescence spectra are collected along the scanning positions of the electron beam across an individual hexagonally cross-sectioned ZnO nanowire to probe the surface effect on the deep-level (DL) emissions of the nanowire. A double-peak feature of DL emission intensity is observed in the intensity versus scanning position when the electron beam scans across the nanowire from one edge to the other. This spatial variation in DL intensity can be well-described by a simple core−shell model considering the strong surface effect. By further quasi-quantitative analysis and comparison with experimental results, we obtained an equivalent surface shell thickness of about 5−6 nm. The result unambiguously confirms that the surface effect plays a key role in the DL emission process of the nanowire, which should be carefully considered and cautiously modified for better performance of nanoscale functional materials and devices.

Introduction

ZnO has received much attention as a promising optical−electronic material because of its wide band gap (3.4 eV), large exciton binding energy (60 meV), good mechanical properties, and high thermal stability. ZnO nanostructures, with high crystallinity and purity, possess abundant morphologies[1−3] and diverse physical properties.[4−6] So far, many applications have been addressed on optical properties of ZnO nanostructures, including ultraviolet light-emitting diodes and laser diodes,[7−9] solar cells,[10] and UV detectors.[11]

Generally, there are two main peaks in the photoluminescence (PL) and cathodoluminescence (CL) spectra of ZnO nanostructures. One is the ultraviolet peak near 380 nm, which is known as the near band edge emission (NBE). The other peak near 500 nm is related to the various deep-level (DL) emissions. Although many defects, including Cu irons,[12] surface hydroxides,[13] oxide antisites,[14] interstitial zinc,[15] and oxygen vacancies,[16,17] have been proposed to account for these DL emissions, the contradiction still exists. Furthermore, the spatial distribution of these defects in ZnO nanostructures has not yet been completely understood. Recently, efforts have been made by post-treatment (e.g., anneal and surface modification) or by tuning the surface-to-volume ratio of ZnO nanostructures to investigate the surface effect on the DL emission.[13,18−20] The results indicate that there is a strong relationship between the DL emission and the surface of the ZnO nanostructures. Among these approaches, however, postannealing[18] or surface modification[13] will either lead to a variation in crystal quality or bring contaminations. Preparing nanoparticles[19] with various diameters will require different synthesis conditions; and for the tapered nanorods,[20] the shrinkage of diameter may also result in nonuniformity in crystal lattice and surface roughness. Therefore, it is still difficult to obtain a confident conclusion on the role of the surface effect on the DL emission of ZnO nanostructures. More reasonable and refined experiments are necessary to unveil the surface effect on the DL emission of the ZnO nanostructures.

In this article, by performing spatially resolved CL, we provide strong experimental evidence of the surface effect on the luminescence of a single uniform ZnO nanowire. The electron beam in CL measurements holds a spot size on the order of 1 nm, which promises high spatial resolution scanning on individual nanostructures. CL spectra from a series of points on an individual uniform ZnO nanowire can be obtained by scanning the beam across it. Because of the hexagonal cross-section of wurtzite ZnO nanowires and the limited penetration depth of an energy-fixed electron beam, the volume ratio of a surface shell to bulk core region can be gradually tuned from point to point in the scanning process. Thus, by acquiring the spatially resolved CL spectra on these points, a correlation between the surface and DL emission intensity was clearly obtained, which confirms that the surface effect plays a crucial role in the DL emission.

Experimental Section

The single crystal ZnO nanowire array is synthesized by a vapor phase transport and condensation method. Details of the preparation are described elsewhere.[21] The as-prepared nanowires are mechanically scratched from the growth substrate and transferred onto a cleaned silicon wafer on which a series of trenches with a 3 μm width and 1 μm depth have been patterned by conventional microprocessing. The nanowires crossed over the trenches are chosen for CL measurement in order to eliminate the influence from the silicon substrate. The morphology and structure of the nanowires are examined by field emission scanning electron microscopy (FESEM), high-resolution transmission electron microscopy (HRTEM), and X-ray

* To whom correspondence should be addressed. (N.P.) E-mail: npan@mail.ustc.edu.cn. Telephone: +86-551-3607048. Fax: +86-551-3606266. (X.W.) E-mail: xpwang@ustc.edu.cn. Telephone: +86-551-3607090. Fax: +86-551-3606266.

† Hefei National Laboratory for Physical Sciences at the Microscale.

‡ Department of Physics.

10.1021/jp903690g CCC: $40.75
Published on Web 06/19/2009

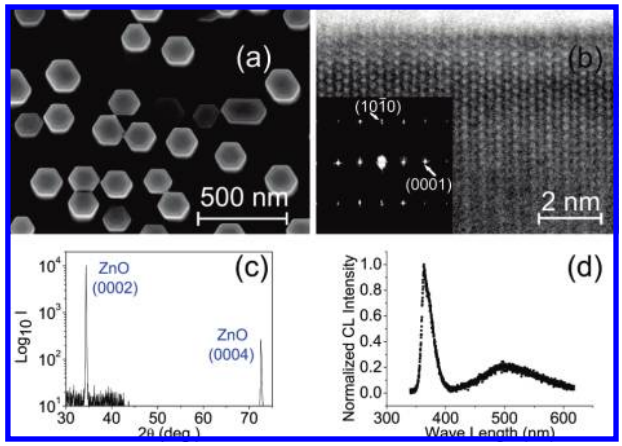

Figure 1. (a) SEM image of the as-prepared ZnO nanowire array. (b) HRTEM image of a ZnO nanowire and the corresponding selected area electron diffraction (SAED) pattern (inset). (c) XRD result of the nanowire array. (d) Typical CL spectrum of a single ZnO nanowire.

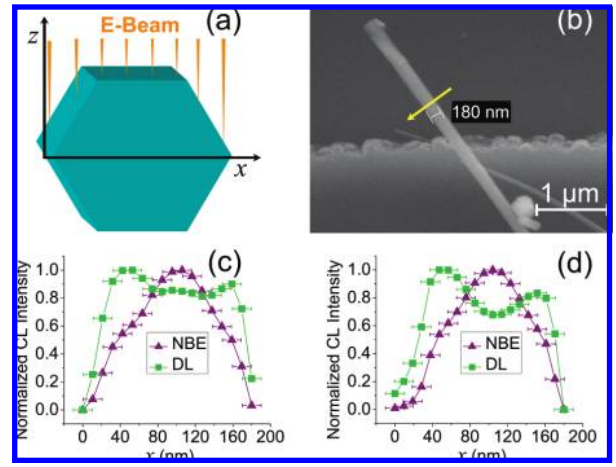

Figure 2. (a) Schematic setup of CL measurements. (b) SEM image of the sample. Yellow line is the path for CL scanning. (c) and (d) Normalized integrated intensities of NBE (purple ▲) and DL emissions (green ■) from the CL scanning under electron acceleration voltages of (c) 3 kV and (d) 4 kV. The *x* axis denotes the position on the ZnO nanowire.

diffraction (XRD). CL spectra are collected by the use of a Gatan Mono-CL3 system attached to a FEI SIRION-200 FESEM, and 3 and 4 kV electron acceleration voltages are used. All spectra are collected at room temperature.

Results and Discussion

Figure 1a shows the SEM image of the as-prepared nanowire array. As shown, the nanowires are vertically well-grown with a diameter ranging from 140 to 200 nm. A hexagonal cross section can be seen clearly. Figure 1b is the HRTEM image of a single nanowire, revealing that there are no obvious defects in the as-prepared nanowire and that the surface of the nanowire is quite clean. Figure 1c is the XRD result of the nanowire array. Only two peaks, namely, (0002) and (0004) of wurtzite ZnO, can be clearly observed, indicating that the nanowires have a high-purity wurtzite ZnO phase as well as good alignment along their *c* axis. Figure 1d is the typical CL spectrum taken from a single nanowire. The two main peaks with central wavelengths near 380 and 500 nm attributed to the NBE and DL emission, respectively, can be clearly observed, which is consistent with previous reports.[20]

In the CL experiment, it is surprising that the intensity of NBE and DL emissions vary notably with the electron beam position scanning on the ZnO nanowire. In order to investigate the origin of this behavior, a series of CL spectra are collected at various positions across the ZnO nanowire. Figure 2a is the schematic setup of the CL measurement. Figure 2b shows the SEM image of a single ZnO nanowire across the trench with a diameter of 180 nm, and the rough edge of the trench can be clearly seen in the image. As depicted in Figure 2a, the spot of the electron beam moves across the nanowire at about a 10 nm distance for each step along the yellow line shown in Figure 2b. At each point, CL spectra are obtained, and the normalized integrated intensities of NBE and DL emissions (I_{NBE} and I_{DL}) at the point can be deduced. I_{NBE} and I_{DL} vary at different positions along the yellow line on the nanowire under the electron acceleration voltage of 3 and 4 kV as plotted in panels c and d of Figure 2, respectively. As shown, the same features can be observed in panels c and d of Figure 2. For the NBE emission, when the electron beam moves from one edge of the nanowire to the other edge along the radial direction (defined as the *x* direction in Figure 2), I_{NBE} first increases gradually, reaches the maximum near the center position of the nanowire, and then decreases as shown by the purple ▲ in panels c and d of Figure 2d. However, for the DL emission, the behavior is rather different. The maximum I_{DL} is not located at the center of the nanowire but occurs near both edges of the nanowire as shown by the green ■ in panels c and d of Figure 2.

By supposing that the NBE emission occurs uniformly in the nanowire, we can well-understand the phenomena of I_{NBE} variation with the scanning position of the electron beam. For the hexagonally cross-sectioned nanowire, its thickness increases from the edge to the center, and I_{NBE} of CL will therefore present the same trend when the electron beam moves from the edge to the center of the nanowires. However, a similar interpretation is not valid for the result of I_{DL} in which two maximums appear near the edges of the nanowire. In our previous work, we found that the DL emission of the ZnO nanostructure depends strongly on the surface property of the nanostructure.[20] Consequently, we believe that the behavior of the I_{DL} variation here is due to the surface effect.

A core−shell model has been first proposed by Shalish et al. to analyze the surface luminescence of ZnO quasi-quantitively,[22] which has been proved efficient to deal with surface-related inhomogeneous emissions in ZnO nanostructures.[20,23] In order to account for the experimental observation of the spatially resolved DL emission intensity curves in panels c and d of Figure 2, we apply a similar simple core−shell model for the ZnO nanowire with a perfect hexagonal cross section (Figure 3) and suppose that the DL emission from the shell region of the nanowire is dominant as compared to that from the core region. It is reasonable to consider that the shell is uniform throughout the nanowire surface with an equivalent thickness, *t*; thus, we can divide the cross section of the nanowire into four regions, I−IV, in which each region has a different volume ratio of the shell to the core. When the electron beam moves from one edge of the nanowire to its center, it first locates exclusively on the shell of the nanowire in region I, resulting in I_{DL} increasing apparently with the increasing volume of the shell. When the beam reaches regions II and III, the DL emission from the core of the nanowire occurs. Note that because of the side facet of the ZnO nanowire being acclivitous, the equivalent surface shell thickness for the electron beam scanning is therefore $t/\sin 30° = 2t$ in region II, and it will decrease from $2t$ to t in region III. The equivalent surface shell thickness maintains at t in region IV. Because the shell region has a

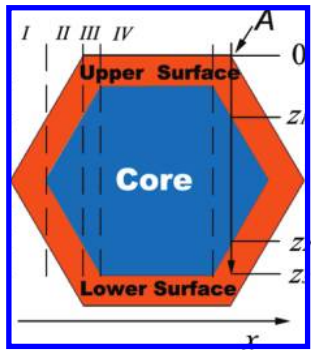

Figure 3. Scheme of the core−shell model. Various regions I−IV are separated by dashed lines. The electron beam moves along the x axis. For scanning point A, z_1 and z_2 are the depths of the upper surface and core regions, respectively, and z_3 is the maximum penetration depth of the electron beam.

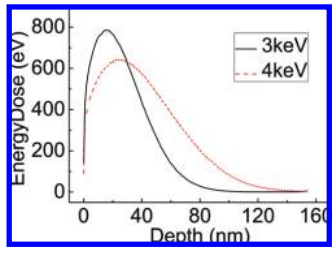

Figure 4. Simulated energy dose profile for a free-standing ZnO nanowire with a 180 nm diameter. Black solid line and red dashed line represent the results under 3 and 4 kV electron acceleration voltages, respectively.

dominant contribution to I_{DL}, the above geometrical feature of the nanowire will result in I_{DL} increasing first and then decreasing, which forms the peaks in panels c and d of Figure 2. In region IV, both contributions from the core and shell regions are maintained as constant, which results in the I_{DL} variation becoming smooth. When the electron beam moves from the center to the other edge of the nanowire, the tendency of I_{DL} variation reverses. The above qualitative analysis is consistent with the experimental observation in Figure 2, indicating that the core−shell model accounting for the DL emission is reasonable.

In the following, we further demonstrate the relationship between I_{DL} (of a single nanowire) and the scanning position (of the electron beam) with consideration of the injected electron distribution in the nanowire. Note that an upper surface, core, and lower surface region are labeled in Figure 3 according to the core−shell model. As shown in Figure 3, under a controlled acceleration voltage, the electrons injected from point A will penetrate vertically into the nanowire to a certain depth and lead to a specific energy profile.[24] Obviously, I_{NBE} and I_{DL} of a nanowire will be dependent on the penetration depth as well as the energy profile of the injected electrons. A Monte Carlo simulation, based on Mott's elastic scattering cross section and Penn's dielectric function, is carried out in order to obtain detailed information on the electron energy dissipation profile.[25,26] Because the CL measurement is preformed exclusively on those positions of the nanowires suspended over the trenches, neither the substrate nor the interface effect is considered in the simulation. The amount of simulated incident electron trajectories is 500000. The simulated energy dose profile is shown in Figure 4, in which the horizontal axis denotes the penetration depth of the injected electron, quantitatively ranging from the upper surface region to the lower one (of the nanowire) defined in Figure 3.

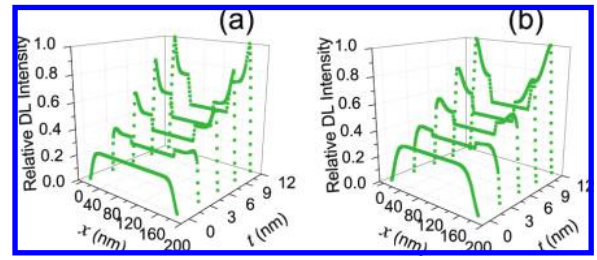

Figure 5. Calculated spatial distribution of relative I_{DL} based on the energy dose profile given in Figure 4 and eq 1 for a series of values of t from 0 to 12 nm. The electron acceleration voltage is (a) 3 kV and (b) 4 kV. t refers to the equivalent surface thickness.

On the basis of the results in Figure 4, the energy profile for electrons injected into the nanowire at various scanning positions can be obtained. For example, when electrons inject from point A marked in Figure 3, the energy dose in the upper surface, core, and lower surface regions can be calculated as $\int_0^{z_1} E(z)dz$, $\int_{z_1}^{z_2} E(z)dz$, and $\int_{z_2}^{z_3} E(z)dz$, where $E(z)$ denotes the energy dose at the specific depth of z. Then the relative I_{DL} excited at scanning point A can be expressed as

$$I_{DL}(A) \propto w_S\left(\int_0^{z_1} E(z)dz + \int_{z_2}^{z_3} E(z)dz + w_B\int_{z_1}^{z_2} E(z)dz \right) \quad (1)$$

where w_S and w_B are the weight of the surface and core recombination contributive to the DL emission, respectively. According to our previous work, the optimized values of w_S and w_B are chosen to satisfy $w_S + w_B = 1$ and $w_S:w_B = 5:1$.[20]

With the energy dose profile obtained in Figure 4 and eq 1, the spatial distribution of I_{DL} can be calculated under the core−shell model with a series values of shell thickness t. Figure 5 shows the spatially resolved I_{DL} distribution for a nanowire with a 180 nm diameter under the electron acceleration voltage of 3 and 4 kV. As shown, for the case without considering shell thickness ($t = 0$), no peak can be observed in the calculated curve of I_{DL} versus position, which is absolutely inconsistent with the experimental results shown in Figure 2. However, for the cases with any non-zero values of t, the curves possess a double-peak feature as the experimental observations. It should be noted that because of the sharp interface existing in the core−shell model, the calculated I_{DL} show a more rapid decrease than that observed when the electron beam moves from region III to region IV. Additionally, the peak value of I_{DL} is found to be proportional to the value of t, indicating that the thickness of the surface shell of the nanowire dramatically affects the DL emission.

By comparing the experimental results (Figure 2) to the calculated ones (Figure 5) with the least-squares method, we can estimate the actual value of t. The shell thickness t for the ZnO nanowire with a 180 nm diameter is found to be 5−6 nm, which is much smaller than the diameter of the nanowire. The t value estimated here is also on the same order of magnitude with our previous study, in which $t = 9.9$ nm for a tapered ZnO nanorod. The trivial difference is probably due to the difference in the synthesis process and morphology. The small value of t further confirms the conclusion that the surface effect plays a dominant role in DL emission. Furthermore, for all of those ZnO nanostructures whose dimensions shrink to ~10 nm or less such as thin films or the side wall of nanotubes, the surface effect might greatly influence their properties as indicated in this study. Therefore, the surface effect would need

to be carefully considered and well-controlled in nanodevices design and application.

Conclusions

In summary, we have investigated the surface effect on the luminescence of single uniform ZnO nanowires by spatially resolved CL measurements. A double-peak feature is observed in the I_{DL} position curve when the electron beam moves across the nanowire. This I_{DL} variation can be well understood by a simple core−shell model under the consideration of the strong surface effect. By comparing the experimental and calculated results, we found an equivalent surface shell thickness of 5−6 nm. The result confirms that the surface effect plays a dominant role in the DL emission process of the nanowire. This surface effect must be considered and controlled properly to optimize the performance of nanostructures and nanodevices.

Acknowledgment. The authors acknowledge financial support from the National Key Basic Research Program (Grant 2006CB922002) and the Natural Science Foundation of China (Grants 50721091, 10874165, 50532040, and 10874160).

References and Notes

(1) Shen, G. Z.; Bando, Y.; Chen, D.; Liu, B. D.; Zhi, C. Y.; Golberg, D. *J. Phys. Chem. B.* **2006**, *110*, 3973.

(2) Pan, N.; Wang, X. P.; Zhang, K.; Hu, H. L.; Xu, B.; Li, F. Q.; Hou, J. G. *Nanotechnology.* **2005**, *16*, 1069.

(3) Matsuu, M.; Shimada, S.; Masuya, K.; Hirano, S.; Kuwabara, M. *Adv. Mater.* **2006**, *18*, 1617.

(4) Anthony, S. P.; Lee, J. I.; Kim, J. K. *Appl. Phys. Lett.* **2007**, *90*, 103107.

(5) Wang, Y. S.; Thomas, P. J.; O'Brien, P. *J. Phys. Chem. B.* **2006**, *110*, 21412.

(6) Choopun, S.; Vispute, R. D.; Noch, W.; Balsamo, A.; Sharma, R. P.; Venkatesan, T.; Iliadis, A.; Look, D. C. *Appl. Phys. Lett.* **1999**, *75*, 3947.

(7) Tsukazaki, A.; Ohtomo, A.; Onuma, T.; Ohtani1, M.; Makino, T.; Sumiya, M.; Ohtani, K.; Chichibu, S. F.; Fuke, S.; Segawa, Y.; Ohno, H.; Koinuma, H.; Kawasaki, M. *Nat. Mater.* **2005**, *4*, 42.

(8) Könenkamp, R.; Word, R. C.; Godinez, M. *Nano. Letter.* **2005**, *5*, 2005.

(9) Bagnall, D. M.; Chen, Y. F.; Zhu, Z.; Yao, T.; Koyama, S.; Shen, M. Y.; Goto, T. *Appl. Phys. Lett.* **1997**, *70*, 2230.

(10) Law, M.; Greene, L. E.; Johnson, J. C.; Saykally, R.; Yang, P. D. *Nat. Mater.* **2005**, *4*, 455.

(11) Emanetoglu, N. W.; Zhu, J.; Chen, Y.; Zhong, J.; Chen, Y. M.; Lu, Y. C. *Appl. Phys. Lett.* **2004**, *85*, 3702.

(12) Garces, N. Y.; Wang, L.; Bai, L.; Giles, N. C.; Halliburton, L. E.; Cantwell, G. *Appl. Phys. Lett.* **2002**, *81*, 622.

(13) Norberg, N. S.; Gamelin, D. R. *J. Phys. Chem. B.* **2005**, *109*, 20810.

(14) Lin, B. X.; Fu, Z. X.; Jia, Y. B. *Appl. Phys. Lett.* **2001**, *79*, 943.

(15) Liu, M.; Kitai, A. H.; Mascher, P. *J. Lumin.* **1992**, *54*, 35.

(16) Kang, H. S.; Kang, J. S.; Kim, J. W.; Lee, S. Y. *J. Appl. Phys.* **2004**, *95*, 1246.

(17) Shan, F. K.; Liu, G. X.; Lee, W. J.; Shin, B. C. *J. Appl. Phys.* **2007**, *101*, 053106.

(18) Shan, F. K.; Liu, G. X.; Lee, W. J.; Lee, G. H.; Kim, I. S.; Shin, B. C. *Appl. Phys. Lett.* **2005**, *86*, 221910.

(19) Xiong, G.; Pal, U.; Garcia Serrano, J. *J. Appl. Phys.* **2007**, *101*, 024317.

(20) Pan, N.; Wang, X. P.; Li, M.; Li, F. Q.; Hou, J. G. *J. Phys. Chem. C.* **2007**, *111*, 17265.

(21) Geng, C. Y.; Jiang, Y.; Yao, Y.; Meng, X. M.; Zapein, J. A.; Lee, C. S.; Lifshitz, Y.; Lee, S. T. *Adv. Funct. Mater.* **2004**, *14*, 589.

(22) Shalish, I.; Temkin, H.; Narayanamurti, V. *Phys. Rev. B.* **2004**, *69*, 245401.

(23) Chen, C. W.; Chen, K. H.; Shen, C. H.; Ganguly, A.; Chen, L. C.; Wu, J. J.; Wen, H. I.; Pong, W. F. *Appl. Phys. Lett.* **2006**, *88*, 241905.

(24) Everhart, T. E.; Hoff, P. H. *J. Appl. Phys.* **1971**, *42*, 5837.

(25) Ding, Z. J.; Wu, Z. Q. *J. Phys. D: Appl. Phys.* **1993**, *26*, 507.

(26) Ding, Z. J.; Shimizu, R. *Scanning.* **1996**, *18*, 92.

JP903690G